

## UNSTEADY FLOW OF CASSON NANOFLUID THROUGH GENERALIZED FOURIER'S AND FICK'S LAW FOR HEAT AND MASS TRANSFER

by

**Ye-Qi WANG<sup>a</sup>, Ahmad SHAFIQUE<sup>b</sup>, Zaib Un NISA<sup>c</sup>,  
Muhammad Imran ASJAD<sup>d</sup>, Mudassar NAZAR<sup>b,e</sup>,  
Mustafa INC<sup>f,g\*</sup>, and Shao-Wen YAO<sup>a</sup>**

<sup>a</sup>School of Mathematics and Information Science, Henan Polytechnic University, Jiaozuo, China

<sup>b</sup>Centre for Advanced Studies in Pure and Applied Mathematics, Bahauddin Zakariya University,  
Multan, Pakistan

<sup>c</sup>Department of Mathematics, Institute of Southern Punjab, Multan, Pakistan

<sup>d</sup>Department of Mathematics, University of Management and Technology, Lahore, Pakistan

<sup>e</sup>School of Mathematical Sciences, University of Science and Technology of China,  
Hefei, Anhui, China

<sup>f</sup>Department of Mathematics, Science Faculty, Firat University, Elazig, Turkey

<sup>g</sup>Department of Medical Research, China Medical University, Taichung, Taiwan

Original scientific paper

<https://doi.org/10.2298/TSCI22S1029W>

*The purpose of this paper to explain the role and importance of fractional derivatives for mass and heat transfer in Casson nanofluids including clay nanoparticles. These particles can be found in water, kerosene, and engine oil. The physical flow phenomena are illustrated using PDE and thermophysical nanoparticle properties, and this paper addresses the Casson fractional fluid along with chemical reaction and heat generation. The heat and mass fluxes are generalized using the constant proportional Caputo fractional derivative. The present flow model are solved semi-analytically using the Laplace transform. We generated several graphs to understand how various flow factors affect velocity. The acquired results reveal that fractional parameters have dual behavior in velocity profiles. Velocity and temperature are also compared to previous studies. Compared to the other fractional derivatives results, field variables and proposed hybrid fractional derivatives showed a more decaying trend. Furthermore, significant results of clay nanoparticles with various base fluids have been obtained.*

**Keywords:** *Casson fluid, clay nanoparticles, heat generation, chemical reaction, constant proportional Caputo, fractional derivative*

### Introduction

The non-Newtonian fluids possess the diverse nature from Newtonian fluids due to their complex rheological properties. Nanofluids have recently emerged as an important area

---

\*Corresponding author, e-mail: minc@firat.edu.tr

in nanotechnology [1-3], attracting physical scientists. Due to their high thermal conductivity, clay nanoparticles play an important role in oil and gas drilling. Khan *et al.* [4] studied the heat transfer model for such flow of clay nanoparticle formed nanofluids. Fractional derivative is the generalization of ordinary derivative by taking the non-integer order of differentiation. Due to its generalized property, the fractional derivative became a practical way of defining heat and mass transfer phenomena. Baleanu and Fernandez [5] described the different types of properties of fractional-calculus operators. Using a Cattaneo constitutive equation along with a Caputo-Fabrizio time-fractional derivative, Hristov [6] started working on transient heat. Baleanu *et al.* [7] described a new fractional operator that combines proportional Caputo and solved various types of examples using constant proportional Caputo (CPC) derivatives. Asjad *et al.* [8] investigated the flow of a Maxwell fluid usually contains clay nanoparticles along with CPC types fractional derivatives. Ahmad *et al.* [9] used novel fractional derivatives (CPC) to obtain analytical solutions of the Casson nanofluid across an infinite vertical plate. Chu *et al.* [10, 11] used Fourier's and Fick's laws to present a model of the differential-type fluid by fractionalized thermal and mass fluxes with CPC derivative.

The primary goal is to expand the work of [4] by using the CPC fractional derivative to explore the Casson fluid of the clay-water base on nanofluids in two vertical parallel plates along with chemical reaction and heat source using generalized thermal and molecular fluxes. The solution of dimensionless differential equations with boundary conditions is semi-analytically solved by utilizing the Laplace transform. The temperature, concentration and velocity distribution results are attained and graphically discussed.

### Formulation of problem

Let us assume allowing the based fluids like water, engine, and kerosene oils to carve up inside the flow of the clay nanoparticles. The plates are acquired along the  $x'$ -axis, with the  $z'$ -axis being chosen randomly. At  $t' < 0$ , the fluid and plates are all at resting along with ambient temperature  $T_0'$ . The plate's temperature at  $z' = d$  rises or falls from  $T_0'$  to  $T_W'$  after  $t' = 0^+$ . Because of a temperature gradient, the fluid begins to move in the  $x$ -direction, resulting in buoyancy forces rised. Due to low Reynolds number, the magnetic field is minimal.

According to the standard Boussinesq's approximation, the governing equations for an unsteady Casson nanofluid flow inside the channel are given by the following form [9, 12, 13]:

$$\rho_{nf} \frac{\partial u_2(z', t')}{\partial t'} = \mu_{nf} \left( 1 + \frac{1}{\lambda} \right) \frac{\partial^2 u_2(z', t')}{\partial z'^2} - \sigma_{nf} B_0^2 u_2(z', t') + g(\rho \beta_T)_{nf} (T' - T_0') + g(\rho \beta_C)_{nf} (C' - C_0') \quad (1)$$

Thermal equation is:

$$(\rho C_P)_{nf} \frac{\partial T'(z', t')}{\partial t'} = - \frac{\partial q_1(z', t')}{\partial z'} + Q_0 (T' - T_0') \quad (2)$$

The generalized Fourier's Law states that [6, 10]:

$$q_1(z', t') = -K_{nf}^{CPC} D_t^\gamma \frac{\partial T'(z', t')}{\partial z'}, \quad 1 \geq \gamma > 0 \quad (3)$$

Diffusion equation:

$$\frac{\partial C^*}{\partial t^*} = -\frac{\partial J_1}{\partial z^*} - K_1(C^* - C_0) \quad (4)$$

The generalized Fick's Law states that [10]:

$$J_1(z^*, t^*) = -D^{\text{CPC}} D_t^\gamma \frac{\partial C^*}{\partial z^*}, \quad 1 \geq \alpha > 0 \quad (5)$$

The initial as well as boundary conditions are:

$$u_2(z^*, 0) = 0, \quad T^*(z^*, 0) = T_0^*, \quad C^*(z^*, 0) = C_0, \quad 0 \leq z^* \leq d \quad (6)$$

$$u_2(0, t^*) = 0, \quad T^*(0, t^*) = T_0^*, \quad C^*(0, t^*) = C_0, \quad t^* > 0 \quad (7)$$

$$u_2(d, t^*) = 0, \quad T^*(d, t^*) = T_w^*, \quad C^*(d, t^*) = C_w, \quad t^* > 0 \quad (8)$$

The dimensionless form of the flow parameters are:

$$\begin{aligned} x = \frac{z^*}{d}, \quad t = \frac{\nu_f t^*}{d^2}, \quad T = \frac{T^* - T_0^*}{T_w^* - T_0^*}, \quad v = \frac{d}{\nu_f} u_2, \quad C = \frac{C^* - C_0}{C_w - C_0}, \quad J_1^* = \frac{J_1}{J} \\ \text{Gm} = \frac{(g\beta_C)_f (C_w - C_0) d^3}{\rho_f \nu_f^2}, \quad \text{Gr} = \frac{(g\beta_T)_f (T_w^* - T_0^*) d^3}{\rho_f \nu_f^2}, \quad M = \frac{B_0^2 d}{\nu_f}, \quad \text{Br} = 1 + \frac{1}{\lambda} \\ q_1^* = \frac{q_1}{q}, \quad Q = \frac{Q_0 d^2}{(\rho C_P)_f \nu_f}, \quad R = \frac{K_1 d^2}{\nu_f}, \quad r_1 = (1 - \phi) + \phi \frac{\rho_s}{\rho_f}, \quad r_2 = \frac{1}{(1 - \phi)^{2.5}} \\ r_3 = (1 - \phi) + \phi \frac{(\rho\beta_T)_s}{(\rho\beta_T)_f}, \quad r_4 = (1 - \phi) + \phi \frac{(\rho\beta_C)_s}{(\rho\beta_C)_f}, \quad r_5 = 1 + \frac{3 \left( \frac{\sigma_s}{\sigma_f} - 1 \right) \phi}{\left( \frac{\sigma_s}{\sigma_f} + 2 \right) - \left( \frac{\sigma_s}{\sigma_f} - 1 \right) \phi} \\ r_6 = (1 - \phi) + \phi \frac{(\rho C_P)_s}{(\rho C_P)_f}, \quad r_7 = \frac{k_s + 2k_f - 2\phi(k_f - k_s)}{k_s + 2k_f + 2\phi(k_f - k_s)}, \quad n_1 = \frac{D(C_w - C_0)}{Jd} \\ n_2 = \frac{qd}{\nu_f (\rho C_P)_f (T_w^* - T_0^*)}, \quad n_3 = \frac{Jd}{(C_w - C_0) \nu_f}, \quad m_1 = \frac{(T_w^* - T_0^*)}{qd} \end{aligned} \quad (9)$$

Using non-dimensional variables of eq. (9) we have:

$$r_1 \frac{\partial v(x, t)}{\partial t} = r_2 \text{Br} \frac{\partial^2 v(x, t)}{\partial x^2} - Mr_5 v(x, t) + r_3 \text{Gr} T(x, t) + r_4 \text{Gm} C(x, t) \quad (10)$$

$$r_6 \frac{\partial T(x, t)}{\partial t} + n_2 \frac{\partial q_1(x, t)}{\partial x} - QT(x, t) = 0 \quad (11)$$

$$-m_1 r_7^{\text{CPC}} D_t^\gamma \frac{\partial T(x,t)}{\partial x} = q_1(x,t), \quad 1 \geq \gamma > 0 \quad (12)$$

$$\frac{\partial C(x,t)}{\partial t} + n_3 \frac{\partial J_1(x,t)}{\partial x} + RC(x,t) = 0 \quad (13)$$

$$-n_1^{\text{CPC}} D_t^\alpha \frac{\partial C(x,t)}{\partial x} = J_1(x,t), \quad 1 \geq \alpha > 0 \quad (14)$$

$$(x,0) = T(x,0) = C(x,0) = 0, \quad x > 0 \quad (15)$$

$$v(0,t) = 0, \quad T(0,t) = 0, \quad C(0,t) = 0, \quad t > 0 \quad (16)$$

$$v(1,t) = 0, \quad T(1,t) = 1, \quad C(1,t) = 1, \quad t > 0 \quad (17)$$

### Thermophysical properties of nanofluid

In this section, thermophysical properties are defined in [4]:

$$\rho_{\text{nf}} = (1-\phi)\rho_f + \phi\rho_s, \mu_{\text{nf}} = \frac{\mu_f}{(1-\phi)^{2.5}}, (\rho C_P)_{\text{nf}} = (1-\phi)(\rho C_P)_f + \phi(\rho C_P)_s$$

$$\frac{k_{\text{nf}}}{k_f} = \frac{k_s + 2k_f - 2\phi(k_f - k_s)}{k_s + 2k_f + 2\phi(k_f - k_s)}, \quad \frac{\sigma_{\text{nf}}}{\sigma_f} = 1 + \frac{3\left(\frac{\sigma_s}{\sigma_f} - 1\right)\phi}{\left(\frac{\sigma_s}{\sigma_f} + 2\right) - \left(\frac{\sigma_s}{\sigma_f} - 1\right)\phi} \quad (18)$$

where  $\mu_{\text{nf}}$ ,  $(\rho C_P)_{\text{nf}}$ ,  $\rho_{\text{nf}}$ ,  $k_{\text{nf}}$ ,  $\sigma_{\text{nf}}$ , and  $\phi$  are the effective dynamic viscosity, heat capacitance, effective density, effective thermal conductivity, effective electrical conductivity, and volume fraction of the clay nanoparticles, respectively. The thermophysical properties of the nano-materials are defined [8] in tab. 1.

**Table 1. Thermophysical properties of nanofluids**

Material	Symbol	$\rho$	$C_P$	$k$	$\beta \times 10^{-5}$	Pr
Clay	Nano particles	6320	531.8	76.5	1.8	–
Water	H <sub>2</sub> O	997	4179	0.613	21	6.2
Kerosine Oil	KO	783	2090	0.145	99	21
Engine Oil	EO	884	1910	0.114	70	500

### Generalization

#### Generalization of thermal diffusion

The fractional form of Fourier's law [6, 10] is from eq. (12) in dimensionless and used in eq. (11), we get:

$$\frac{\partial T(x,t)}{\partial t} = \frac{r_7}{r_6 Pr} D_t^\gamma \frac{\partial^2 T(x,t)}{\partial x^2} + QT(x,t) \quad (19)$$

where

$${}^{CPC}D_t^\gamma f(x, t)$$

indicates the CPC fractional derivative of  $f(x, t)$  [7] as:

$${}^{CPC}D_t^\gamma f(x, t) = \frac{1}{\Gamma(1-\gamma)} \int_0^t [k_1(\gamma) f(x, \tau) + k_0(\gamma) f'(x, \tau)] (t-\tau)^{-\gamma} d\tau, \quad k_0, k_1 \in (0, 1) \quad (20)$$

#### Generalization of molecular diffusion

The fractional form of Fick's Law [10] is used from eq. (14) into eq. (13), we obtain:

$$\frac{\partial C(x, t)}{\partial t} = \frac{1}{Sc} {}^{CPC}D_t^\alpha \frac{\partial^2 C(x, t)}{\partial x^2} - RC(x, t) \quad (21)$$

#### Solution of problem

The initial boundary value problem for energy, diffusion, and momentum, eqs. (10), (19), and (21) via the technique of Laplace transform can be solved numerically by using Stehfest's as well as Tzou's algorithms [14, 15] in the case of a complex expression.

#### Solution of temperature

The eq. (19) is solved the subject to the conditions stated in eqs. (15)-(17) via Laplace transform method for temperature as:

$$\bar{T}(x, q) = \frac{e^{\sqrt{\frac{r_6 Pr(q-Q)}{r_7 \left( \frac{K_1(\gamma)}{q} + K_0(\gamma) \right) q^\gamma}}}}{q \left[ e^{\sqrt{\frac{r_6 Pr(q-Q)}{r_7 \left( \frac{K_1(\gamma)}{q} + K_0(\gamma) \right) q^\gamma}}}} - 1 \right]} \left[ e^{x \sqrt{\frac{r_6 Pr(q-Q)}{r_7 \left( \frac{K_1(\gamma)}{q} + K_0(\gamma) \right) q^\gamma}}} - e^{-x \sqrt{\frac{r_6 Pr(q-Q)}{r_7 \left( \frac{K_1(\gamma)}{q} + K_0(\gamma) \right) q^\gamma}}}} \right] \quad (22)$$

#### Solution of concentration

The solution of eq. (21) is subject to the conditions given in eqs. (15)-(17) via Laplace transform method for concentration species as:

$$\bar{C}(x, q) = \frac{e^{\sqrt{\frac{Sc(q+R)}{\left( \frac{K_1(\alpha)}{q} + K_0(\alpha) \right) q^\alpha}}}}{q \left[ e^{\sqrt{\frac{Sc(q+R)}{\left( \frac{K_1(\alpha)}{q} + K_0(\alpha) \right) q^\alpha}}} - 1 \right]} \left[ e^{x \sqrt{\frac{Sc(q+R)}{\left( \frac{K_1(\alpha)}{q} + K_0(\alpha) \right) q^\alpha}}} - e^{-x \sqrt{\frac{Sc(q+R)}{\left( \frac{K_1(\alpha)}{q} + K_0(\alpha) \right) q^\alpha}}} \right] \quad (23)$$

### Solution of velocity

The solution of the velocity field of eq. (10) is subject to initial and boundary conditions (15)-(17); by using Laplace transform, we get:

$$\bar{v}(x, q) = \left[ \left[ \frac{r_3 Gr}{r_2 Br} \left( \frac{e^{\sqrt{a_2}}}{q(e^{2\sqrt{a_2}}) - 1} \left( \frac{e^{\sqrt{a_2}} - e^{-\sqrt{a_2}}}{a_2 - a_1} \right) \right) \right] + \left[ \frac{r_4 Gm}{r_2 Br} \left( \frac{e^{\sqrt{a_3}}}{q(e^{2\sqrt{a_3}}) - 1} \left( \frac{e^{\sqrt{a_3}} - e^{-\sqrt{a_3}}}{a_3 - a_1} \right) \right) \right] \right] \times$$

$$\times \left[ \frac{e^{(-x+1)\sqrt{a_1}}}{1 - e^{2\sqrt{a_1}}} + \frac{e^{(x+1)\sqrt{a_1}}}{e^{2\sqrt{a_1}} - 1} \right] - \left[ \frac{r_3 Gr}{r_2 Br} \left[ \frac{e^{\sqrt{a_2}}}{q(e^{2\sqrt{a_2}}) - 1} \left( \frac{e^{x\sqrt{a_2}} - e^{-x\sqrt{a_2}}}{a_2 - a_1} \right) \right] \right] -$$

$$- \left[ \frac{r_4 Gm}{r_2 Br} \left[ \frac{e^{\sqrt{a_3}}}{q(e^{2\sqrt{a_3}}) - 1} \left( \frac{e^{x\sqrt{a_3}} - e^{-x\sqrt{a_3}}}{a_3 - a_1} \right) \right] \right] \quad (24)$$

where

$$a_1 = \frac{r_5 M + q r_1}{r_2 Br}, \quad a_2 = \frac{r_6 Pr(q - Q)}{r_7 \left( \frac{K_1(\gamma)}{q} + K_0(\gamma) \right) q^\gamma}, \quad a_3 = \frac{Sc(q + R)}{\left( \frac{K_1(\gamma)}{q} + K_0(\gamma) \right) q^\gamma}$$

### Result and discussion

This paper investigates clay nanoparticles in Casson fluid along with CPC fractional derivative. The semi-analytical results of velocity, concentration, and temperature are ob-

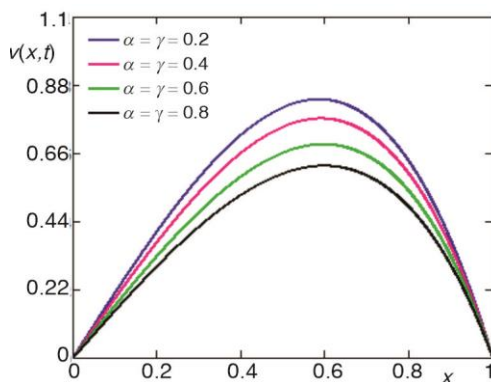


Figure 1. Velocity profile  $v(x,t)$  for fractional parameters  $\alpha = \gamma$  for small time at:  $Gr = 8$ ,  $Q = 0.3$ ,  $Gm = 14$ ,  $M = 0.3$ ,  $Pr = 6.2$ , and  $R = 0.5$

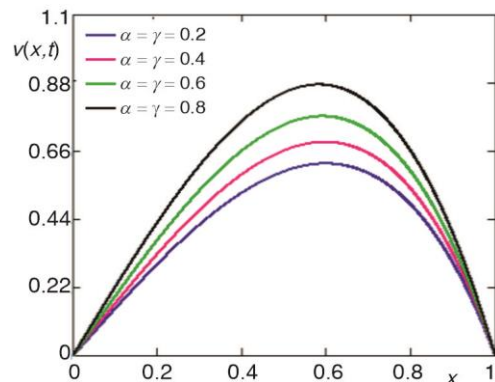
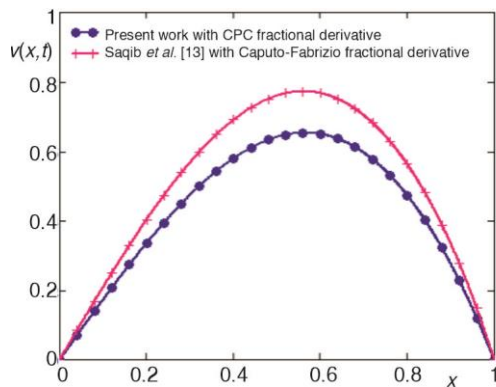


Figure 2. Velocity profile  $v(x,t)$  for fractional parameters  $\alpha = \gamma$  for large time at:  $Gr = 8$ ,  $Q = 0.3$ ,  $Gm = 14$ ,  $M = 0.3$ ,  $Pr = 6.2$ , and  $R = 0.5$

tained. Furthermore, some graphs are positioned to represent the physical effect of the involved parameters, particularly the influence of nanoparticles and fractional parameters.

The fractional parameter reveals the dual nature of the velocity for longer and shorter times. For a shorter period of time, a velocity distribution showed an downward trend and boundary layers decreases with the increasing values of  $\alpha = \gamma$  as depicted in fig. 1. Its behavior is opposite for a longer times as shown in fig. 2. Figure 4 illustrates the velocity distribution contrast for three distinct types of base fluids (kerosene, engine oil, and water). For other applications see [12, 16-18] references.



**Figure 3.** Comparison of velocity profiles between CPC and Caputo-Fabrizio fractional derivatives for  $\alpha = 0.5$ ,  $\beta_b = Gm = 0$ , and  $1/\lambda \rightarrow 0$

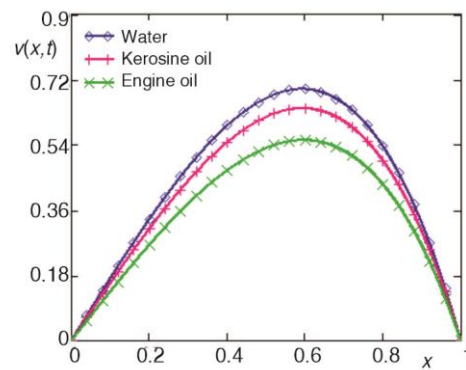


**Figure 4.** Comparison of velocity profile with different base fluids at  $GR = 8$ ,  $Q = 0.3$ ,  $Gm = 14$ , and  $\lambda = 3$

A comparison is drawn among different fluids for fixed value of volume fraction. The velocity of the water-based clay nanofluid is higher than that of the engine oil- and kerosene-based clay nanofluid fluids, respectively. Because water has a higher heat

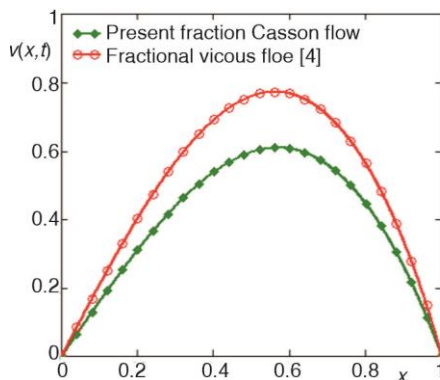


**Figure 5.** Comparison of velocity profile of fractional Casson fluid with viscous fluid [4]

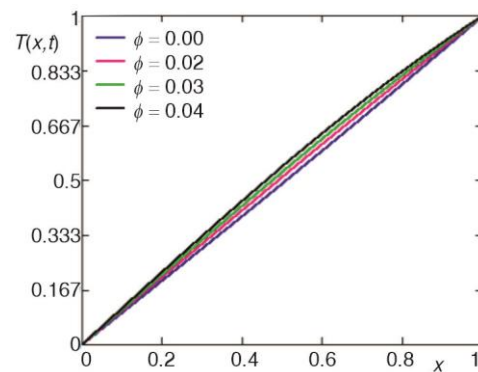


**Figure 6.** Temperature profile  $T(x,t)$  for volume fraction  $\phi$  at  $\alpha = \gamma = 2$ ,  $Q = 3$ , and  $Pr = 6.2$

conductivity than both oils. Figure 5 compares the velocity between the CPC fractional derivative and Khan *et al.* [4]. Because the velocity used in [4] refers to a viscous fluid, whereas the velocity in this study refers to a Casson fluid. Because Casson fluids are thicker than viscous fluids. The graphical behavior of the parameter volume fraction  $\phi$  is represented in fig. 6. The temperature rises when values of volume fraction  $\phi$  are exceeded, as seen in the figure. The volume fraction  $\phi$  of clay nanoparticles rises due to the thermal conductivity of nanofluid.

Figure 3 represents the velocity comparison between CPC fractional derivative with Caputo-Fabrizio fractional derivative used in Saqib *et al.* [13].

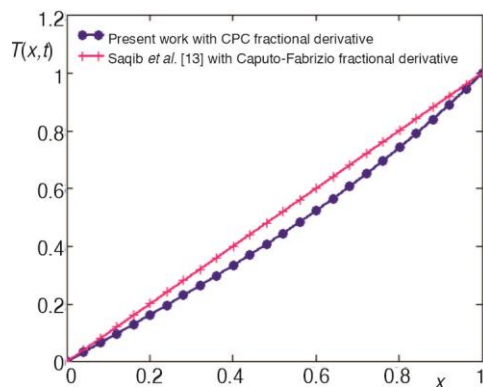


Figure 7. Comparison of temperature profiles between CPC and Caputo-Fabrizio fractional derivatives for  $\alpha = \gamma = 0.5$  and  $1/\lambda \rightarrow 0$

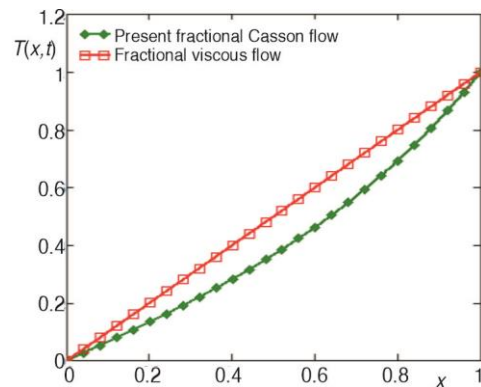


Figure 8. Comparison of temperature profile of fractional Casson fluid with viscous fluid [4]

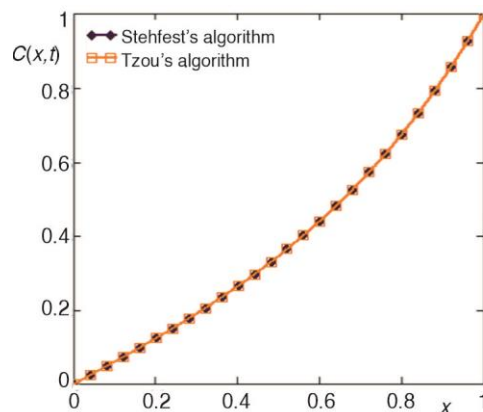


Figure 9. Concentration obtain by Stehfest's [15] and Tzou's [14] algorithms

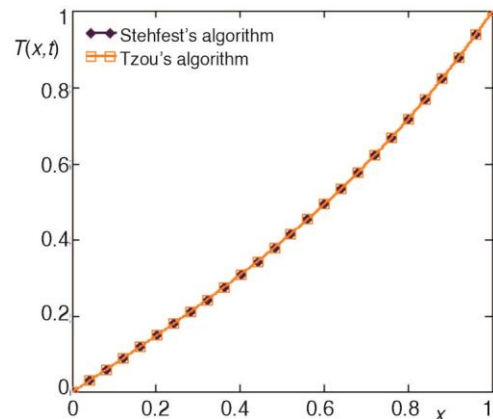


Figure 10. Temperature obtain by Stehfest's [15] and Tzou's [14] algorithms

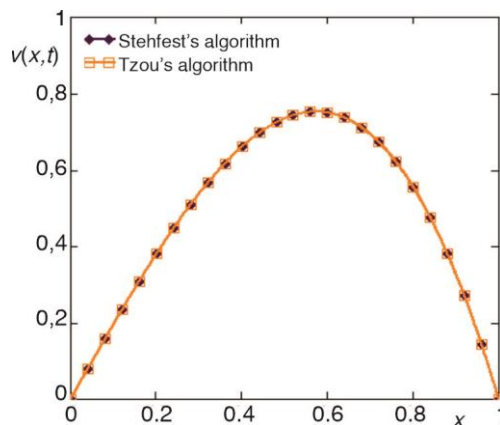


Figure 11. Velocity obtain by Stehfest's [15] and Tzou's [14] algorithms

The comparison of temperature in fig. 7 demonstrate the current work with the fractional derivative Caputo Fabrizio being used by Saqib *et al.* [13].

When  $\beta_b = 0$  and  $\lambda \rightarrow \infty$  in Saqib *et al.* [13], temperature as well as velocity with CPC decrease faster (more decaying nature) than temperature as well as velocity using Caputo-Fabrizio fractional derivative. The temperature comparisons of the CPC fractional derivative with Khan *et al.* [4] are shown in fig. 8. The authenticity of inversion algorithms for concentration distributions as represented in fig. 9. The authenticity of inversion algorithms for temperature distributions as presented in fig. 10 by using [14, 15]. The velocity distributions overlap which shows the authenticity of inversion algorithms as presented in fig. 11.

## Conclusions

A hybrid fractional derivative is used in model of Casson nanofluid along with clay nanoparticles. The velocity, concentration, and temperature fields are determined by solving this flow model semi-analytically. To demonstrate the influencing parameters, multiple graphs of optimizing fields are plotted. The following are outcomes of this flow model.

- Instead of oil-based drilling fluids, water-based drilling nanofluids have the highest velocity.
- Due to fractional parameters, fluid velocity has a dual behavior. Fluid velocity increases for a long time by raising the value of the fractional parameter  $\alpha = \gamma$  but behaves in the opposite way for a shorter time.
- The temperature distribution increases by higher values of volume fraction,  $\phi$ .

## Funding

National Natural Science Foundation of China (No. 71601072), the Fundamental Research Funds for the Universities of Henan Province (No. NSFRF210314) and Innovative Research Team of Henan Polytechnic University (No. T2022-7).

## References

- [1] Wang, F., *et al.*, Unsteady Thermal Transport Flow of Casson Nanofluids with Generalized Mittag-Leffler Kernel of Prabhakar's Type, *Journal of Materials Research and Technology*, 14 (2021), Sept.-Oct., pp. 1292-1300
- [2] Shah, Z., *et al.*, Radiative MHD Casson Nanofluid Flow with Activation Energy and Chemical Reaction Over Past Nonlinearly Stretching Surface Through Entropy Generation, *Scientific Reports*, 10 (2020), 4402
- [3] Zheng, Y., *et al.*, An Investigation on the Influence of the Shape of the Vortex Generator on Fluid Flow and Turbulent Heat Transfer of Hybrid Nanofluid in a Channel, *Journal of Thermal Analysis and Calorimetry*, 143 (2021), Feb., pp. 1425-1438
- [4] Khan, I., *et al.*, Convective Heat Transfer in Drilling Nanofluid with Clay Nanoparticles: Applications in Water Cleaning Process, *Bio-Nano Science*, 9 (2019), Mar., pp. 453-460
- [5] Baleanu, D., Fernandez, A., On Fractional Operators and their Classifications, *Mathematics*, 7 (2019), 9, pp. 830-839
- [6] Hristov, J., Transient Heat Diffusion with a Non-Singular Fading Memory: From the Cattaneo Constitutive Equation with Jeffrey Kernel to the Caputo-Fabrizio Time Fractional Derivative, *Thermal Science*, 20 (2016), 2, pp. 757-762
- [7] Baleanu, D., *et al.*, On a Fractional Operator Combining Proportional and Classical Differintegrals, *Mathematics*, 8 (2020), 3, pp. 360-372
- [8] Asjad, M. I., *et al.*, Application of Water Based Drilling Clay.Nanoparticles in Heat Transfer of Fractional Maxwell Fluid Over an Infinite Flat Surface, *Scientific Reports*, 11 (2021), 18833
- [9] Ahmad, M., *et al.*, Analytical solutions for free convection flow of Casson nanofluid over an infinite vertical plate, *AIMS Mathematics*, 6 (2021), 3, pp. 2344-2358

- [10] Chu, Y.-M., *et al.*, Fractional Model of Second Grade Fluid Induced by Generalized Thermal and Molecular Fluxes with Constant Proportional Caputo, *Thermal Science*, 25 (2021), Special Issue 2, pp. S207-S212
- [11] Chu, Y.-M., *et al.*, Heat Transfer Flow of Maxwell Hybrid Nanofluids due to Pressure Gradient Into Rectangular Region, *Scientific Reports*, 10 (2020), 1, 16643
- [12] Asadullah, M., *et al.*, Mathematical Fractional Modeling of Transpot Phenomena of Viscous Fluid-Flow Between Two Plates, *Thermal Science*, 25 (2021), Special Issue 2, pp. 417-421
- [13] Saqib, M., *et al.*, Application of Fractional Differential Equations to Heat Transfer in Hybrid Nanofluid: Modeling and Solution Via Integral Transforms, *Advances in Difference Equations*, 2019 (2019), 52
- [14] Tzou, D. Y., *Macro to Microscale Heat Transfer, the Lagging Behavior*, 2<sup>nd</sup> ed., Taylor and Francis, Washington DC, USA, 1997, pp. 01-339
- [15] Stehfest, H., Algorithm 368: Numerical Inversion of Laplace Transform, *Communication of Advanced Composit Material*, 13 (1970), 1, pp. 47-49
- [16] Menni, Y., *et al.*, Heat and mass transfer of oils in baffled and finned ducts, *Thermal Science*, 24 (2021), Suppl. 1, pp. S267-276
- [17] Arshed, S., *et al.*, Soliton Solutions for Non-Linear Kudryashov's Equation via Three Integrating Schemes, *Thermal Science*, 25 (2021), Special Issue 2, pp. S157-S163
- [18] Ulutas, E., *et al.*, Exact Solutions Of Stochastic Kdv Equation With Conformable Derivatives In White Noise Environment, *Thermal Science*, 25 (2021), Special Issue 2, pp. S143-S149